Electronic Supplementary Material (ESI) for Dalton Transactions.
This journal is © The Royal Society of Chemistry 2021

Supporting Information

Temperature-induced irreversible phase transition of a water-stable open-framework Zinc phosphate and its water-assisted high proton conduct

Jing-Wei Yu, [a] Hai-Jiao Yu, [a] Qiu Ren, [a] Jin Zhang, [a] Yang Zou,*[a] Hong-Bin Luo, [a] Lifeng Wang, [b] Xiao-Ming Ren*[a,c]

[a] State Key Laboratory of Materials-Oriented Chemical Engineering and College of Chemistry and Molecular Engineering, Nanjing Tech University, Nanjing 211816, P. R. China

[b] Institute for Frontier Materials (IFM), Deakin University, 75 Pigdons Road, Waurn Ponds, Victoria 3216, Australia

[c] State Key Laboratory of Coordination Chemistry, Nanjing University 210023, P. R. China

Tel: +86-25-58139476

E-mail: zouyang@njtech.edu.cn (YZ); xmren@njtech.edu.cn (XMR)

Contents

X-ray crystallography

Table S1. Crystallographic data and structural refinements for **α** and **β**

Table S2. Selected Bond Lengths (Å) and Bond Angles (°) for **α** and **β**.

Table S3. Distances [Å]and angles [°] of selected hydrogen bonding for **α**.

Table S4. Distances [Å]and angles [°] of selected hydrogen bonding for **β**.

Figure S1. Asymmetric unit with atom labelling (a) **α** $N(CH_3)_4{\cdot}Zn(HPO_4)(H_2PO_4)$, (b) **β** $N(CH_3)_4ZnH_3(PO_4)_2$.

Figure S2. The open framework with 12-ring channels and H-bond (yellow dash lines) in the crystal of **α**.

Figure S3. The open framework with 12-ring channels and H-bond (yellow dash lines) in the crystal of **β**.

Figure S4. TGA of **α** and **β** under nitrogen atmosphere.

Figure S5. Experimental (Cu-Kα1 radiation) and simulated powder XRD patterns for (a) **α**, (b) **β**.

Calculation of ion conductivity from Impedance spectra by fitting with equivalent circuit (RQ) Q

Scheme S1. Equivalent circuit (RQ)Q.

Table S5. Table of fitting parameters to determine the conductivity of **α** measured under N_2 atmosphere in various temperatures using ZSimpWin software.

Table S6. Table of fitting parameters to determine the conductivity of **β** measured under N_2 atmosphere in various temperatures using ZSimpWin software.

Table S7. Table of fitting parameters to determine the conductivity of **α** measured under various RH at room temperature (20 °C) using Gamry Echem Analyst software.

Table S8. Table of electronic conductivity of **α** measured under 98%RH in various temperatures using Gamry Echem Analyst software.

Table S9. Table of fitting parameters to determine the conductivity of **β** measured under various RH at room temperature (20 °C) using Gamry Echem Analyst software.

Figure S6. Nyquist plots of **α** measured under N_2 atmosphere (anhydrous environment) at selected temperatures.

Figure S7. Nyquist plots of **β** measured under N_2 atmosphere (anhydrous environment) at selected temperatures.

Figure S8. (a) Temperature-dependent proton conductivity of **β** measured under N_2 atmosphere (anhydrous environment), (b) Plot of ln(σT) against 1000/T (Ea = 0.92 eV).

Figure S9. Humidity-dependent proton conductivity of **α** and **β** measured at room temperature.

Figure S10. PXRD patterns of **α** and **β** (**α** after the conductivity measurement, which was carried out in the 98% RH for about 3 days).

Reagents and materials

All solvents and reagents were analytical grade and used without further purification: 85% phosphoric acid from Shanghai Lingfeng Chemical Reagent Co., Ltd. Zinc oxide and 25% tetramethylammonium hydroxide solution from sinopharm group Co., Ltd. Deionized water was purified using a Milli-Q filtering system.

X-ray crystallography

Single crystal X-ray diffraction data for **α** and **β** were collected at 273.15 K and 301.01K using graphite monochromated Mo/Ka radiation (λ=0.71073 Å) on a Bruker D8 QUEST Apex III CCD area detector diffractometer. Data reduction and absorption corrections were performed with the SAINT [1] and SADABS [2] software packages, respectively. The structures were solved by a direct method using the SHELXL-2014/7 software package. [3]

The non-hydrogen atoms were anisotropically refined using the full-matrix least-squares method on F2. The hydrogen atoms of $[NMe_4]^+$ cations were generated geometrically, the other hydrogen atoms were located on a difference Fourier map. CCDC 2048790 (α) and 2048791 (β) contain the supplementary crystallographic data for this paper. The details about data collection, structural refinement and crystallography are listed in Table S1.

Table S1. Crystallographic data and structural refinements for **α** and **β**.

Formula	$C_8H_{31}N_2O_{16}P_4Zn_2$ (**α**)	$C_8H_{22}N_2O_{16}P_4Zn_2$ (**β**)
Formula weight	665.97	656.89
CCDC no.	2048790	2048791

Temperature (K)	273.15	301.01
Wavelength (Å)	0.71073	0.71073
Crystal size/mm	0.20 × 0.15 × 0.08	0.12 × 0.08 × 0.05
Crystal system	Monoclinic	Orthorhombic
Space group	*Pc* (No. 7)	*Fdd*2 (No. 43)
a/Å	8.4561(8)	15.987(14)
b/Å	13.7954(14)	9.949(8)
c/Å	10.1880(11)	15.258(8)
α/(°)	90	90
β/(°)	90.872(3)	90
γ/(°)	90	90
V/Å^3	1188.3(2)	2427(3)
Z	2	4
F(000)	682.0	1327.0
$\theta_{min,max}$/°	2.49–27.42	4.685–27.661
GOF	1.110	1.186
R_1,[a] wR_2 [b] [I > 2σ(I)]	0.0521, 0.1403	0.0309，0.0896

Table S2. Selected Bond Lengths (Å) and Bond Angles (°) for **α** and **β**.

α	**Bond Lengths**			**β**	**Bond Lengths**
Zn(1)-O(1)^{i}	1.913(8)	Zn(2)-O(6)	1.932(8)	Zn(1)-O(1)	1.937(4)
Zn(1)-O(3)	1.919(7)	Zn(2)-O(9)	1.911(7)	Zn(1)-O(1)^{iv}	1.937(4)
Zn(1)-O(5)	1.946(8)	Zn(2)-O(10)^{ii}	1.956(8)	Zn(1)-O(2)	1.943(4)
Zn(1)-O(13)	1.936(8)	Zn(2)-O(15)^{iii}	1.929(8)	Zn(1)-O(2)^{iv}	1.943(4)
P(1)-O(1)	1.503(8)	P(3)-O(13)	1.498(8)	P(1)-O(1)^{v}	1.504(4)
P(1)-O(2)	1.533(10)	P(3)-O(14)	1.542(8)	P(1)-O(2)	1.517(4)
P(1)-O(3)	1.507(8)	P(3)-O(15)	1.510(8)	P(1)-O(3)	1.577(5)
P(1)-O(4)	1.573(10)	P(3)-O(16)	1.608(9)	P(1)-O(4)	1.549(4)
P(2)-O(5)	1.522(8)	P(4)-O(9)	1.505(8)		
P(2)-O(6)	1.515(8)	P(4)-O(10)	1.500(9)		
P(2)-O(7)	1.602(9)	P(4)-O(11)	1.555(9)		
P(2)-O(8)	1.544(8)	P(4)-O(12)	1.570(10)		
α	Bond Angles			**β**	Bond Angles
O(1)^{i}-Zn(1)-O(3)	108.3(3)	O(6)-Zn(2)-O(10)^{ii}	109.2(4)	O(1)^{iv}-Zn(1)-O(1)	106.1(3)
O(1)^{i}-Zn(1)-O(5)	106.8(4)	O(9)-Zn(2)-O(6)	116.3(4)	O(1)^{iv}-Zn(1)-O(2)^{iv}	113.70(18)
O(1)^{i}-Zn(1)-O(13)	107.8(4)	O(9)-Zn(2)-O(10)^{ii}	100.7(4)	O(1)-Zn(1)-O(2)^{iv}	106.39(19)
O(3)-Zn(1)-O(5)	114.2(4)	O(9)-Zn(2)-O(15)^{iii}	109.2(4)	O(1)-Zn(1)-O(2)	113.70(18)

O(3)-Zn(1)-O(13)	111.4(4)	O(15)^{iii}-Zn(2)-O(6)	109.8(4)	O(1)^{iv}-Zn(1)-O(2)	106.39(19)
O(13)-Zn(1)-O(5)	108.2(4)	O(15)^{iii}-Zn(2)-O(10)^{ii}	111.3(4)	O(2)-Zn(1)-O(2)^{iv}	110.7(3)
O(1)-P(1)-O(2)	106.5(5)	O(13)-P(3)-O(14)	110.8(5)	O(1)^{v}-P(1)-O(2)	112.5(3)
O(1)-P(1)-O(3)	112.8(5)	O(13)-P(3)-O(15)	112.9(5)	O(1)^{v}-P(1)-O(3)	110.2(3)
O(1)-P(1)-O(4)	108.8(5)	O(13)-P(3)-O(16)	109.8(5)	O(1)^{v}-P(1)-O(4)	109.3(2)
O(2)-P(1)-O(4)	106.5(7)	O(14)-P(3)-O(16)	106.1(5)	O(2)-P(1)-O(3)	108.6(2)
O(3)-P(1)-O(2)	110.9(6)	O(15)-P(3)-O(14)	110.7(5)	O(2)-P(1)-O(4)	112.2(3)
O(3)-P(1)-O(4)	111.1(5)	O(15)-P(3)-O(16)	106.3(5)	O(4)-P(1)-O(3)	103.8(3)
O(5)-P(2)-O(7)	105.0(5)	O(9)-P(4)-O(11)	105.5(5)		
O(5)-P(2)-O(8)	111.6(4)	O(9)-P(4)-O(12)	106.6(5)		
O(6)-P(2)-O(5)	110.6(5)	O(10)-P(4)-O(9)	116.2(5)		
O(6)-P(2)-O(7)	110.3(5)	O(10)-P(4)-O(11)	110.8(6)		
O(6)-P(2)-O(8)	111.2(5)	O(10)-P(4)-O(12)	111.3(5)		
O(8)-P(2)-O(7)	107.9(5)	O(11)-P(4)-O(12)	105.7(6)		

Symmetry transformations used to generate equivalent atoms:

^{i}=x, -y, -1/2+z; ^{ii}=x, -1-y, 1/2+z; ^{iii}=1+x, y, z; ^{iv}=-x, 1-y, z; ^{v}=1/4-x, 1/4+y, 1/4+z;

Table S3. Distances [Å]and angles [˚] of selected hydrogen bonding for **α**

D-H…A	d(D-H)	d(H..A)	d(D…A)	<D-H…A
O2-- H2…O14	0.8200	1.8400	2.638(12)	166.00
O4-- H4…O8	0.8200	1.8700	2.654(12)	161.00
O7-- H7…O14#1	0.8200	1.8400	2.636(10)	165.00
O11-- H11…O8#2	0.8200	1.8400	2.574(10)	148.00
O14-- H14…O12#3	0.8200	1.8300	2.609(10)	158.00
O16-- H16…O8	0.8200	1.9300	2.656(10)	147.00
C2-- H2C…O5#4	0.9600	2.5700	3.446(14)	152.00
C5-- H5A…O13#5	0.9600	2.6000	3.537(15)	167.00
C7-- H7C…O16	0.9600	2.5800	3.426(15)	147.00

Symmetry operators: #1: 1+x,y,z; #2: x,-1-y,-1/2+z; #3: -1+x,-1-y,1/2+z; #4: -1+x,y,1+z; #5: x,-1-y,1/2+z.

Table S4. Distances [Å]and angles [°] of selected hydrogen bonding for **β**

D-H…A	d(D-H)	d(H..A)	d(D…A)	<D-H…A
O4-- H4…O4#1	0.8200	1.6500	2.435(7)	159.00

Symmetry operators: #1: -x,1-y,z.

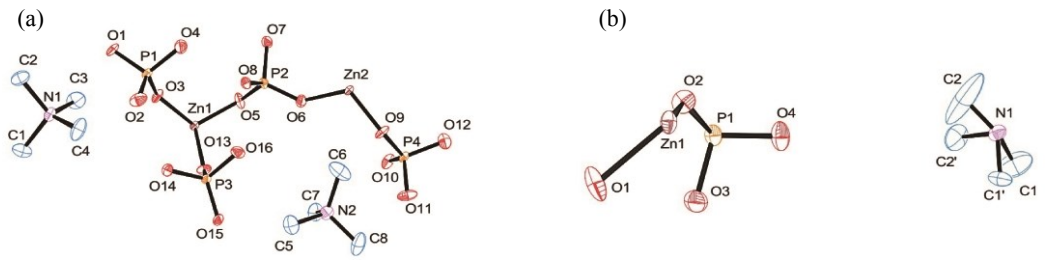

Figure S1. Asymmetric unit with atom labelling (a) **α** $N(CH_3)_4{\cdot}Zn(HPO_4)(H_2PO_4)$, (b) **β** $N(CH_3)_4$ $.ZnH_3(PO_4)_2$.

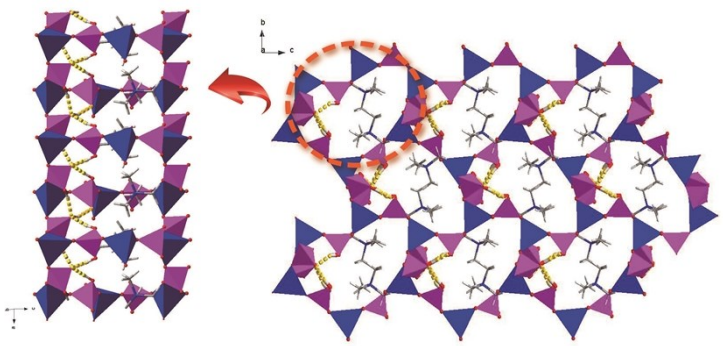

Figure S2. The open framework with 12-ring channels and H-bond (yellow dash lines) in the crystal of **α**.

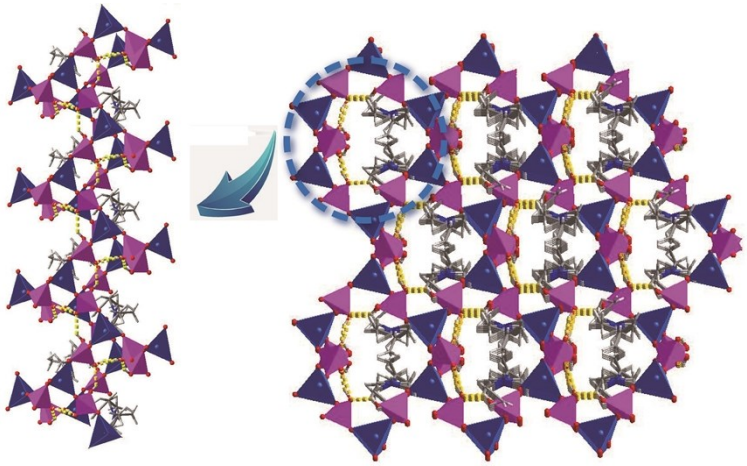

Figure S3. The open framework with 12-ring channels and H-bond (yellow dash lines) in the crystal of **β**.

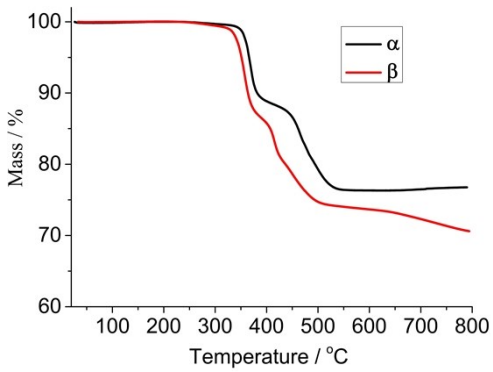

Figure S4. TGA of **α** and **β** under nitrogen atmosphere.

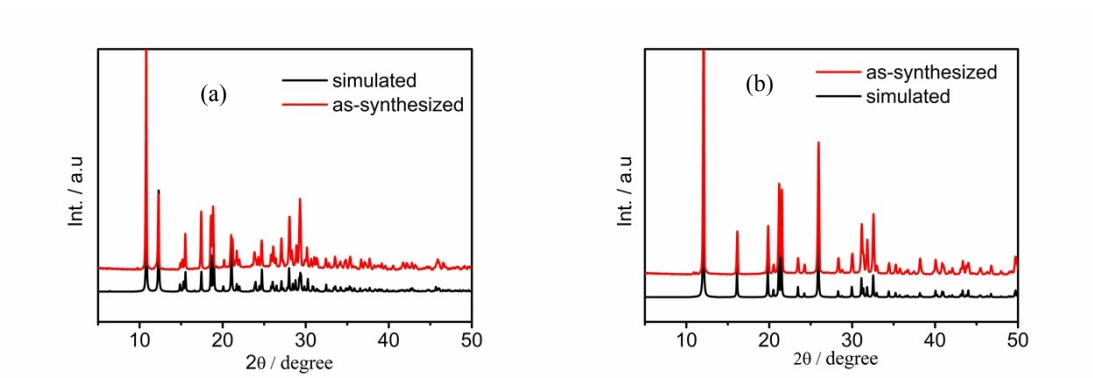

Figure S5. Experimental (Cu-Kα1 radiation) and simulated powder XRD patterns for (a) **α**, (b) **β**.

Calculation of ion conductivity from Impedance spectra by fitting with equivalent circuit (RQ) Q

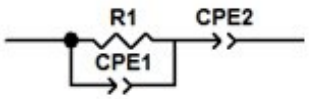

Scheme S1. Equivalent circuit (RQ)Q.

The possible behaviour of the electrode-electrolyte interfaces can be discussed in terms of blocking or non-blocking character. An interface is blocking concerning the given charge-carrying species in the electrolyte if those species cannot cross the interface or exchange charge (in the electron form) with the electrode; otherwise, it is non-blocking with respect to the given species. For the EIS tests with blocking electrodes, the equivalent circuits are shown in Scheme 1, where R1 represents the bulk resistance, while CPE1 and CPE2 are the constant phase elements for the non-ideal capacitance behaviour of bulk and electrodes, respectively. [4, 5] It consists of the contributions of the bulk and the electrodes, as is reflected in the Nyquist plot that involves a high-frequency semicircle and a low-frequency tail. The bulk resistance R1 can be estimated by either fitting to the equivalent circuit or by the method of low-frequency minimum/intercept along the real Z-axis.

Here we provide the values of R1 by fitting the experimentally obtained data points along with the curve generated by the equivalent circuit mentioned above. The conductivity (σ) was calculated using the equation of σ = L/RS, where the symbols σ, R, L and S represent the conductivity, resistance, thickness and cross-sectional area of the sample, respectively.

On the basis of the structural analysis (Figure S2), hydrogen bonding is formed between the phosphate groups. The proton conduction mechanism is generally identified by the activation energy (Ea) [6]. According to the Arrhenius plots, the calculated Ea of α in 443-493K temperature region is 0.58 eV , Ea around the Tc is 2.8eV, and Ea of β in the 293-353K temperature region is 0.92 eV. In addition, the Ea values of the α were similar to those of anhydrous proton conductors [7]. These results suggested that the proton conduction under N_2 atmosphere (anhydrous

environment) was based on a mechanism without the assistant of water molecules. The possible mechanisms of proton conduction in α may follow both the vehicle and Grotthuss mechanisms in which $[NMe_4]^+$ ions may act as the proton carriers for the proton conduction.

Table S5. Table of fitting parameters to determine the conductivity of **α** measured under N_2 atmosphere in various temperatures using ZSimpWin software

Temp. (K)	Value of R1 (Ω)	rel. std. error (%)	Conductivity (Scm^{-1})	χ^2 value
293	9.53E+08	31.41	3.27E-10	3.69E-03
303	6.35E+08	26.62	4.91E-10	4.52E-03
313	6.21E+08	65.43	5.02E-10	4.89E-03
323	4.77E+08	51.61	6.54E-10	4.33E-03
333	3.21E+08	30.74	9.72E-10	4.05E-03
343	1.76E+08	15.79	1.77E-09	4.05E-03
353	8.93E+07	7.514	3.49E-09	3.22E-03
363	4.08E+07	4.605	7.64E-09	3.02E-03
373	1.39E+07	5.71	2.24E-08	1.36E-03
383	3.34E+06	8.557	9.35E-08	6.72E-03
393	5.65E+05	3.187	5.52E-07	3.30E-03
403	4.50E+04	1.611	6.94E-06	1.30E-03
413	8.87E+03	1.325	3.52E-05	1.02E-03
423	4.29E+03	1.061	7.28E-05	6.38E-04
433	2.57E+03	0.983	1.22E-04	5.88E-04
443	1.72E+03	0.856	1.81E-04	4.91E-04
453	1.39E+03	0.711	2.25E-04	3.96E-04
463	1.25E+03	0.540	2.49E-04	2.63E-04
473	1.16E+03	0.340	2.68E-04	1.27E-04
483	1.09E+03	0.235	2.86E-04	7.20E-05

Table S6. Table of fitting parameters to determine the conductivity of **β** measured under N_2 atmosphere in various temperatures using ZSimpWin software.

Temp. (K)	Value of R1 (Ω)	rel. std. error (%)	Conductivity (Scm^{-1})	χ^2 value
293	3.66E+08	15.73	4.91E-10	3.96E-02
303	1.09E+08	11.03	1.65E-09	4.24E-02

313	3.37E+07	8.483	5.33E-09	3.86E-02
323	1.17E+07	6.868	1.54E-08	3.25E-02
333	4.53E+06	5.694	3.97E-08	2.62E-02
343	1.99E+06	4.83	9.05E-08	2.07E-02
353	9.58E+05	4.171	1.88E-07	1.62E-02
363	5.07E+05	3.674	3.55E-07	1.27E-02
373	2.87E+05	3.27	6.26E-07	9.92E-03
383	1.71E+05	2.913	1.05E-06	7.68E-03
393	1.10E+05	2.582	1.64E-06	5.99E-03
403	7.29E+04	2.249	2.47E-06	4.68E-03
413	5.01E+04	1.923	3.58E-06	3.63E-03
423	3.56E+04	1.621	5.05E-06	2.83E-03
433	2.60E+04	1.348	6.92E-06	2.19E-03
443	1.93E+04	1.115	9.31E-06	1.68E-03
453	1.46E+04	0.936	1.23E-05	1.31E-03
473	8.47E+03	0.737	2.12E-05	9.19E-04
483	6.29E+03	0.696	2.85E-05	8.47E-04
493	4.43E+03	0.607	4.05E-05	6.72E-04

Table S7. Table of fitting parameters to determine the conductivity of **α** measured under various RH at room temperature (25 °C) using Gamry Echem Analyst software.

RH(%)	Value of R1 (Ω)	Error(Ω)	Conductivity (Scm^{-1})	Goodness of Fit
68	7.13E+03	38.27	3.83E-05	3.77E-04
75	3.87E+03	20.13	7.05E-05	4.45E-04
85	2.48E+03	12.99	1.10E-04	1.48E-04
95	669.6	3.297	4.08E-04	4.23E-04
98	62.73	11.66	4.35E-03	4.90E-03

Table S8. Table of electronic conductivity of **α** measured under 98%RH in various temperatures using Gamry Echem Analyst software.

Temp (K)	Value of R1 (Ω)	Error(Ω)	Conductivity (Scm^{-1})	Goodness of Fit

293	65.05	0.699	4.20E-03	1.07E-02
298	51.4	0.466	5.31E-03	4.90E-03
303	44.9	3.109	6.09E-03	9.68E-03
308	38.3	0.258	7.13E-03	1.22E-02
313	32.79	0.192	8.32E-03	1.82E-02
318	29.24	2.571	9.34E-03	1.68E-02
323	24.48	0.362	1.12E-02	2.07E-02
328	22.02	0.144	1.24E-02	2.19E-02
333	21.56	0.169	1.27E-02	2.33E-02

Table S9. Table of fitting parameters to determine the conductivity of **β** measured under various RH at room temperature (25 °C) using Gamry Echem Analyst software.

RH(%)	Value of R1 (Ω)	Error(Ω)	Conductivity (Scm^{-1})	Goodness of Fit
68	3.50E+04	422.3	1.06E-05	1.13E-03
75	1.94E+04	122.9	1.92E-05	4.13E-04
85	7.22E+02	3.724	5.15E-04	1.12E-04
95	152	7.70E-01	2.45E-03	4.62E-04
98	10.81	6.96E-02	3.44E-02	4.32E-02

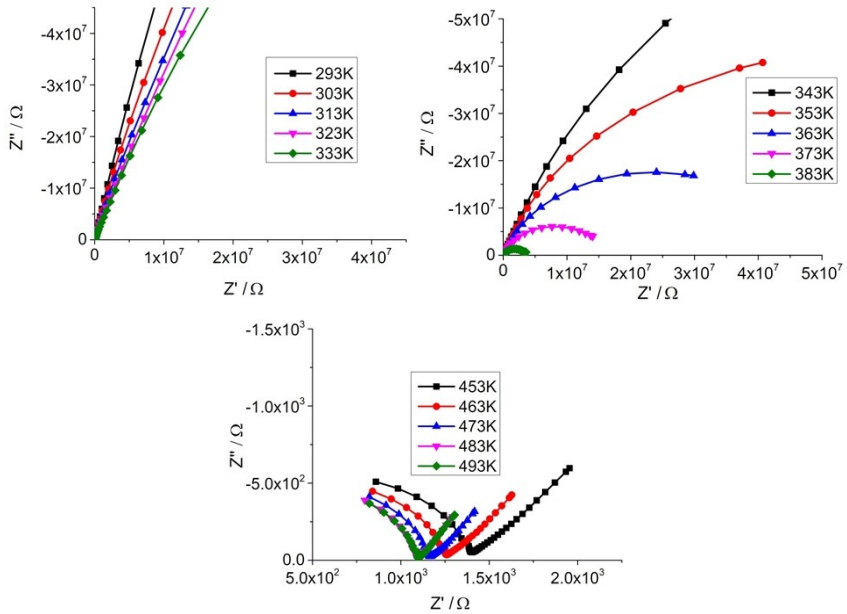

Figure S6. Nyquist plots of **α** measured under N_2 atmosphere (anhydrous environment) at selected temperatures.

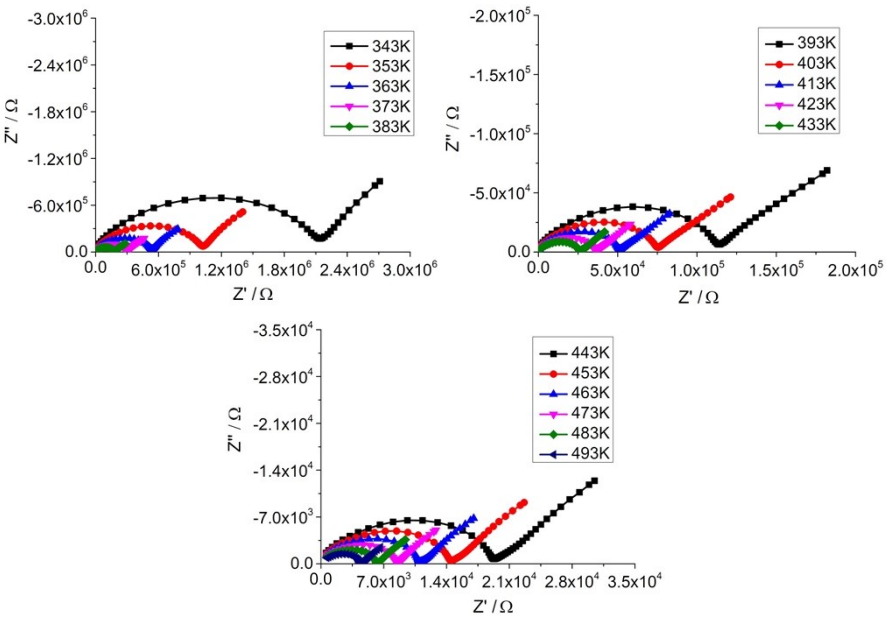

Figure S7. Nyquist plots of **β** measured under N_2 atmosphere (anhydrous

environment) at selected temperatures.

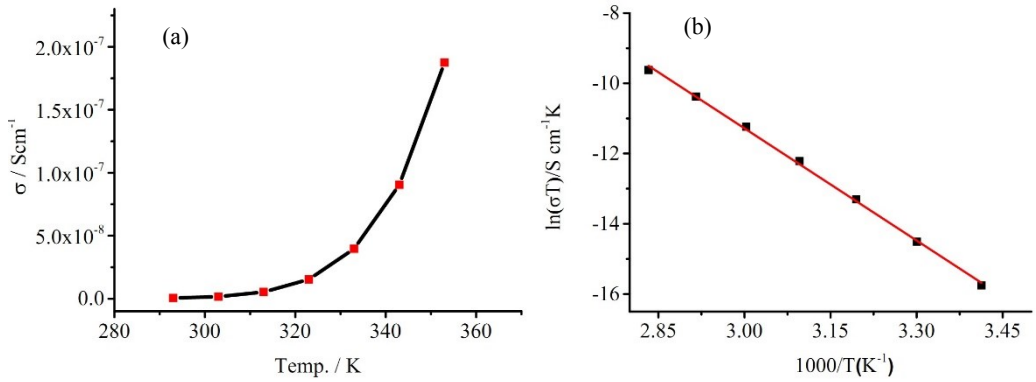

Figure S8. (a) Temperature-dependent proton conductivity of **β** measured under N_2 atmosphere (anhydrous environment). (b) Plot of ln(σT) against 1000/T (Ea = 0.92 eV).

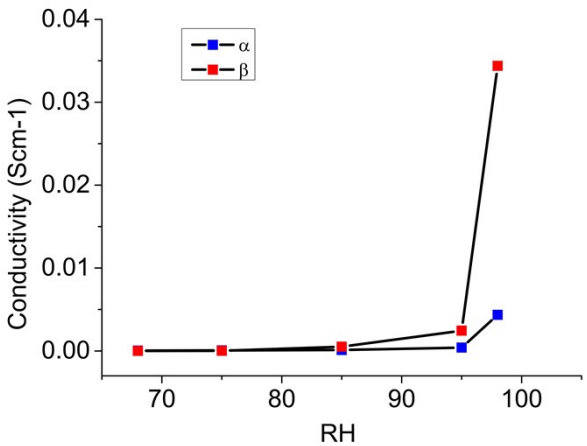

Figure S9. Humidity-dependent proton conductivity of **α** and **β** measured at room temperature.

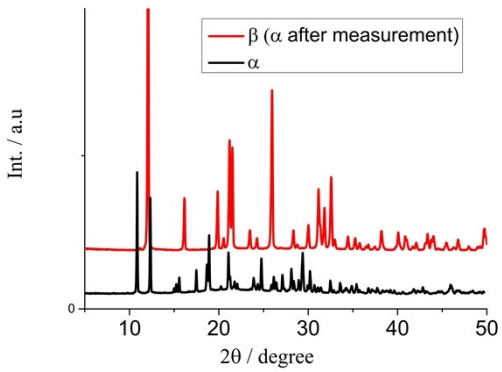

Figure S10. PXRD patterns of **α** and **β** (**α** after the conductivity measurement, which was carried out in the 98% RH for about 3 days).

REFERENCES

[1] Bruker, APEX 2, SAINT, XPREP, Bruker AXS Inc., Madison,Wisconsin, USA, 2007.

[2] Bruker, SADABS, Bruker AXS Inc., Madison,Wisconsin, USA, 2001.

[3] G. M. Sheldrick, Crystal Structure Refinement with SHELXL. *Acta Crystallogr. Sect. C Struct. Chem.* 2015, **71** (1), 3–8.

[4] E. Barsoukov, J.R. Macdonald, Impedance Spectroscopy: Theory, Experiment, and Applications, John Wiley & Sons Inc, New York, 2005.

[5] J. A. Hurd, R. Vaidhyanathan, V. Thangadurai, C. I. Ratcliffe, I. L. Moudrakovski, G. K. H. Shimizu, *Nat. Chem.* 2009, 1 , 705–710.

[6] P. Ramaswamy, N.E. Wong, G.K.H. Shimizu, Chem. Soc. Rev. 2014, 43, 5913–5932.

[7] a) M. Yamada and I. Honma, J. Phys. Chem. B, 2004, 108, 5522–5526; b) M. Yamada and K. Tanoue RSC Adv., 2019, 9, 36416–36423.